Psychostimulant Drugs Activate Cell-type Specific and Topographic cFos Expression in the Lumbar Spinal Cord

Pauline Tarot, Laia Castell, Yuki Nakamura, Coline Rulhe, Juri Aparicio Arias, Laura Cutando, Federica Bertaso, Denis Hervé, Emmanuel Valjent

Psychostimulant drugs activate cell-type specific and topographic cFos expression in the lumbar spinal cord

Pauline Tarot[1], Laia Castell[1], Yuki Nakamura[2,3,4], Coline Rulhe[1], Juri Aparicio Arias[1], Laura Cutando[1,5], Federica Bertaso[1], Denis Hervé[2,3,4], Emmanuel Valjent[1]

[1]IGF, University of Montpellier, CNRS, Inserm, Montpellier 34094, France

[2]Inserm UMR-S 1270, Paris 75005, France

[3]Sorbonne Université, Faculty of Sciences and Engineering, Paris 75005, France

[4]Institut du Fer à Moulin, 17 rue du Fer à Moulin, Paris 75005, France

[5]Institut de Neurociències and Department of Cell Biology, Physiology and Immunology, Universitat Autònoma de Barcelona, Bellaterra, Spain

* Correspondence should be addressed to: Emmanuel Valjent (emmanuel.valjent@igf.cnrs.fr), IGF, University of Montpellier, CNRS, Inserm, Montpellier 34094, France

Running title:

Psychostimulant-evoked neuronal ensembles in spinal cord

Number of pages: 30

Number of figures: 6

Number of tables: 3

Highlights

- D-amphetamine induces pS32-cFos in lumbar spinal cord
- Increased pS32-cFos occurs in both inhibitory and excitatory neurons in the lumbar spinal cord
- Blockade of dopamine transporter induces pS32-cFos in lumbar spinal cord
- Increased pS32-cFos by psychostimulants is independent of locomotion

Abstract

Psychostimulant drugs, such as cocaine, d-amphetamine and methylphenidate, alter a wide range of behaviors including locomotor activity and somatosensory perception. These altered behaviors are accompanied by the activation of specific neuronal populations within reward-, emotion- and locomotion-related circuits. However, whether such regulation occurs at the level of the spinal cord, a key node for neural circuits integrating and coordinating sensory and motor functions has never been addressed. By evaluating the temporal and spatial expression pattern of the phosphorylated form of the immediate early gene cFos at Ser32 (pS32-cFos), used as a proxy of neuronal activation, we demonstrate that, in adult male mice, d-amphetamine increases pS32-cFos expression in both inhibitory and excitatory neurons in dorsal and ventral horns at the lumbar spinal cord level. Interestingly, a fraction of neurons activated by a first exposure to d-amphetamine can be re-activated following d-amphetamine re-exposure. Similar expression patterns were observed in response to cocaine and methylphenidate, but not following morphine and dozilcipine administration. Finally, the blockade of dopamine reuptake was sufficient to recapitulate the increase in pS32-cFos expression induced by psychostimulant drugs. Our work provides evidence that cFos expression can be activated in lumbar spinal cord in response to acute psychostimulants administration.

Keywords: psychostimulants, spinal cord, dopamine, cFos-immunoreactive neurons

Introduction

Motor behaviors require the activation of spatially distributed and interconnected neural networks in the forebrain, brainstem and spinal cord (Grillner and El Manira, 2020). The sequential recruitment of specific circuits along this axis allows the selection, initiation, execution and termination of motor actions with precision. Drugs exacerbating dopamine (DA) and norepinephrine release profoundly affect the fine-tuning control of motor behaviors. Indeed, a single exposure to psychostimulant drugs such as d-amphetamine, cocaine or methylphenidate enhances motor behaviors whose manifestations depend on the dose administered (Gaytan et al., 1998; Yates et al., 2007). At low doses, these drugs stimulate fast exploratory activity characterized by an increase in locomotion and rearing (Yates et al., 2007; Ztaou et al., 2021). However, at high doses, psychostimulants promote a variety of repetitive behaviors ranging from in-place stereotypies (continuous sniffing, circling, intense grooming, and self-gnawing) to patterned locomotion and continuous up-and-down rearing motion often accompanied by intermittent episodes of wall licking (Yates et al., 2007; Ztaou et al., 2021).

The broad motor repertoire induced by psychostimulants is highly correlated with neuronal activation within the striatum, a brain structure densely innervated by midbrain DA neurons and involved in selecting and initiating motor actions (Canales and Graybiel, 2000). Indeed, specific patterns of neuronal activation classically identified by evaluating the expression pattern of immediate early genes are recruited following acute exposure to psychostimulants (Berke et al., 1998; Graybiel et al., 1990; Moratalla et al., 1993). For instance, cocaine or methylphenidate induce a widespread expression of the proto-oncogene cFos in striosomal and matrix compartments in both sensorimotor and limbic striatal domains (Canales and

Graybiel, 2000; Graybiel et al., 1990). In contrast, d-amphetamine increases cFos levels prominently in striosomes, a pattern of expression highly predictive of the intensity of motor stereotypies (Canales and Graybiel, 2000). Psychostimulant exposure also enhances cFos immunoreactivity in the pedunculopontine nucleus and the cuneiform nucleus, two brainstem excitatory nuclei of the mesencephalic locomotor region regulating motor behaviors (Geisler et al., 2008). However, psychostimulants-induced neuronal activation within executive spinal motor circuits have never been investigated.

In the present study, we take advantage of an immediate early gene-based method to characterize neuronal populations activated in the spinal cord in response to a single exposure to d-amphetamine. By using a variety of reporter mouse lines, we investigated the cell-type specific identity of amphetamine-induced cFos expression. We finally assessed the ability of different classes of locomotor-stimulating drugs to trigger neuronal activation in the lumbar spinal cord.

Materials and methods

Animals

Male C57BL/6 (n = 65) from Charles River Laboratories, *Gad67-eGFP* (Tg(Gad2-eGFP)DJ31Gsat) (n = 3), *GlyT2-eGFP* (Tg(Slc6a5-eGFP)1Uze) (n = 4), *VGluT2-RiboTag* (n = 3) and *Fos-Trap* (n = 9) mice were used in the present study. *Vglut2-Ribotag* mice were generated by crossing *VGluT2-Cre* (Tg(Slc17a6-icre)1Oki) and *RiboTag* (Sanz et al., 2009) mice and *Fos-Trap* were generated by crossing *Fos-2A-iCreER* (Allen et al., 2017) and *R26-Trap* (Liu et al., 2014) mice. Male 8- to 12-week old mice (25-30 gr) were used in the current study. All mice were housed in groups of 2 to 5 per cage (standard sizes according to the European animal welfare guidelines 2010/63/EU) and maintained in a 12h light/dark cycle (lights on from 7:00 am to 7:00 pm), in stable conditions of temperature (22°C) and humidity (60%), with food and water provided *ad libitum*. In all experiments, arbitrary assignments were used to allocate mice to specific treatments. No randomization was performed to allocate subjects in the study. All animal procedures were conducted in accordance with the guidelines of the French Agriculture and Forestry Ministry for handling animals (authorization number/license B34-172-41) and approved by the relevant local and national ethics committees (authorizations APAFIS#15092 and APAFIS#26765).

Drugs and treatment

Drugs, drug doses and routes are detailed in Table 1. All drugs were administered at doses inducing known behavioral and/or molecular responses in mice (Gangarossa et al., 2019; Valjent et al., 2010). For *in vivo* pharmacological experiments, mice were habituated to handling and saline injections three consecutive days before the experiments. Drugs were dissolved in 9 g/L NaCl (saline) and administered on day 4.

All the mice were injected in the home cage and perfused 90 min after injection except for the time-course experiment for which mice were also perfused at 30, 60, and 120 min after d-amphetamine administration. None of these manipulations were classified as painful or invasive.

Fos-Trap experiments

4-hydroxytamoxifen (4-OHT, H6278, Sigma-Aldrich, Saint-Quentin Fallavier, France) was dissolved in 1 ml ethanol (100%). Corn oil (C8267, Sigma-Aldrich) was then added and ethanol was evaporated by incubating the open tubes at 50°C overnight in the dark. The volume of corn oil was adjusted for injecting the dose of active drug at 10 ml/kg. 4-OHT was administered i.p. at the dose of 50 mg/kg of active Z form. D-amphetamine sulfate (Sigma-Aldrich) was dissolved in 0.9% (w/v) NaCl (saline) and injected i.p. (10 mg/kg). During the 6 days preceding treatments, *Fos-Trap* mice were habituated to the experimental conditions in the aim to limit the *Fos* gene induction by novelty. The first day, animals were just handled for 5 min. The next 2 days, they were handled and pricked in the abdomen with a syringe needle without injection. At day 4, mice were handled and received one injection of saline. The following two days, they received 2 injections of saline solution in the left and right sides of the abdomen. After each manipulation, the animals were immediately placed back in their home cage. On day 7, mice received an injection of 4-OHT (50 mg/kg, i.p.) and immediately after, 5 of them were administered with d-amphetamine (10 mg/kg, i.p.) and the 4 others with saline solution. After injections, mice were returned to their home cage. Seven days later, all the mice were treated with d-amphetamine (10 mg/kg, i.p.).

Tissue preparation and immunofluorescence

Ninety minutes after drugs administration (or at 30, 60, 90, 120 minutes for the time course experiments), mice were anaesthetized with Euthasol (TVM lab, France) at a dose (340 mg/kg) allowing rapid, efficient and deep anesthesia, which constitute a prerequisite to avoid the dephosphorylation of proteins (Gangarossa et al., 2019). Mice were then transcardially perfused (every 7 min by alternating groups) with 40 g/L paraformaldehyde prepared in 0.1M sodium phosphate buffer (pH 7.5). Spinal cords were extracted, post-fixed overnight in the same solution and stored at 4°C. The lumbar segments were then included in 4% agarose and 40-µm thick sections were cut using a vibratome (Leica VT 1000S, France). Slices were stored at -20°C in a solution containing 30% (vol/vol) ethylene glycol, 30% (vol/vol) glycerol, and 0.1M sodium phosphate buffer, until they were processed for immunofluorescence (Bertran-Gonzalez et al., 2008). Lumbar sections were identified using the Allen Mouse Spinal Cord Atlas (mousespinal.brain-map.org). Free-floating sections were rinsed three times (10 min/wash) in Tris-buffered saline (TBS, 50 mM Tris-HCl, 150 mM NaCl, pH 7.5) before 15 min of incubation in 0.2% (vol/vol) Triton X-100 in TBS. Sections were then rinsed three times (10 min/wash) in TBS before 60 min blocking in a solution of 3% BSA in TBS. Sections were incubated for 72 h at 4°C with the primary antibodies (Table 2) diluted in a TBS solution containing 1% BSA and 0.15% Triton X-100 (Puighermanal et al., 2015). Following three rinses of 10 min in TBS, sections were incubated for 45 min at 4°C with the secondary antibodies: goat Cy3-coupled anti-rabbit (1:500, Jackson Immuno-Research, Cat# 111-165-003), goat Alexa Fluor 488-coupled anti-chicken (1:500, Thermo Fisher Scientific, Cat# A-11039), and goat Alexa Fluor 488-coupled anti-mouse (1:500, Thermo Fisher Scientific, Cat# A-11001). Following incubation with secondary antibodies, sections were rinsed twice

for 10 min in TBS. Mounting was performed using DPX (Sigma-Aldrich, Saint-Quentin Fallavier, France). Confocal microscopy was carried out at the Montpellier RIO Imaging Facility. Single or double-immunolabeled images were single confocal sections acquired using sequential laser scanning confocal microscopy (Leica SP8 or Zeiss LSM780). pS32-cFos-positive cells were pseudocolored in red while GFP-, HA-, CB-, PV- and CR-immunoreactive cells were pseudocolored in green.

Quantification

Cells were considered positive for a given marker only when the nucleus was clearly visible (Bertran-Gonzalez et al., 2008). Quantification was performed manually taking as standard reference a fixed threshold of fluorescence. Histograms in Figures 1, 3, 4, 5 and 6, represent the number of neurons averaged from 3 to 4 lumbar sections. Histograms in Figures 2 and 3 show the co-expression of pS32-cFos/markers as percentage of pS32-cFos- and GFP-immunoreactive neurons respectively, in the distinct laminae of the lumbar spinal cord. Numbers of positive neurons summed from 3 to 4 lumbar sections per mice are reported in Table 3.

Statistical analysis

Data were analyzed using one-way ANOVA or Student *t*-test. Significance threshold was set at $p < 0.05$. One-way ANOVA analysis was followed by Šidák's multiple comparisons test.

Results

Immediate early gene expression-based method is a widely used approach to characterize neuronal activation at the regional and cellular level. Here we tested the ability of various psychostimulant drugs to recruit specific neuronal populations in the lumbar spinal cord by analyzing the spatio-temporal and molecular distribution of cells expressing the phosphorylated form of cFos at Ser32 (pS32-cFos), a post-translational modification associated with an increased stability, nuclear localization and activity of cFos (Sasaki et al., 2006).

Acute d-amphetamine increases pS32-cFos expression in lumbar spinal cord

We first investigated whether d-amphetamine promoted neuronal activation in the mouse lumbar spinal cord. To do so, the number of pS32-cFos-immunoreactive neurons was quantified in lamina I to X of the lumbar spinal cord 30, 60, 90 and 120 min after a single intraperitoneal administration of d-amphetamine (10 mg/kg) (**Figure 1**). In saline-treated mice (90 min post-injection), few pS32-cFos-positive neurons (<20 cells) were detected in lamina II, III, VI and VII (**Figure 1a-b**). This pattern remained unchanged 30 min after d-amphetamine injection (**Figure 1a-b**). However, the analysis of pS32-cFos expression at 60, 90 and 120 min revealed a gradual increase in pS32-cFos-positive neurons in the dorsal and ventral horns, notably in lamina III ($F_{4, 10} = 5.997$, $p = 0.01$), and IV ($F_{4, 10} = 4.597$, $p = 0.023$), V ($F_{4, 10} = 20.3$, $p < 0.0001$), VI ($F_{4, 10} = 35.83$, $p < 0.0001$), VII ($F_{4, 10} = 26.79$, $p < 0.0001$), VIII ($F_{4, 10} = 25.58$, $p < 0.0001$) and X ($F_{4, 10} = 10.7$, $p = 0.0012$) (**Figure 1a-b**). No significant changes were detected in laminae I ($F_{4, 10} = 0.7929$, $p = 0.5559$) and II ($F_{4, 10} = 4.282$, $p = 0.0283$) whatever the time points analyzed following d-amphetamine administration (**Figure 1a-b**). Moreover, no cFos-positive cells were

found in lamina IX where motor neurons are located (**Figure 1a-b**). These results indicate that a single injection of d-amphetamine evokes specific neuronal activation in the dorsal (laminae V and VI) and the ventral horns (laminae VII and VIII) of the lumbar spinal cord.

D-amphetamine activates both inhibitory and excitatory neurons in the lumbar spinal cord

To determine whether d-amphetamine-induced lumbar spinal cord neuronal activation occurred preferentially in inhibitory and/or excitatory neurons, pS32-cFos expression was monitored in *Gad67-eGFP*, *GlyT2-eGFP* and *VGluT2-Ribotag* mice, which allow the immunohistological identification of GABAergic, glycinergic and glutamatergic neurons, respectively (**Figure 2**). Based on the kinetics of pS32-cFos expression (**Figure 1a**), all the subsequent analyses were performed in mice perfused 90 min after d-amphetamine administration. First, we analyzed the distribution of pS32-cFos-immunoreactive neurons in *Gad67-eGFP* mice, which express the green fluorescent protein (GFP) under the control of the *Gad67* promoter (GABAergic neurons) (**Figure 2a**). Our analysis revealed that the highest percentage of pS32-cFos cells co-expressing GFP was found in the superficial laminae (~35% in lamina I; ~18% in lamina II; ~25% in lamina III and ~15% in lamina IV) and in the lamina X surrounding the central canal (~14%) (**Figure 2a-b**). In contrast, low or no pS32-cFos/GFP co-expressing cells was detected in lamina V (~2%), VI (~1%), VII (~5%), VIII (~5%) and IX (0) (**Figure 2a-b**). These results indicate that d-amphetamine-induced pS32-cFos expression occurs in a small fraction of *Gad67*-expressing neurons.

A distinct cell type-specific pattern of pS32-cFos/GFP-positive neurons was observed when the analysis was performed in *GlyT2-eGFP* mice that allow the identification of glycinergic neurons (**Figure 2c-d**). Indeed, percentages of pS32-cFos/GFP-immunoreactive cells were high in laminae activated in response to d-amphetamine reaching ~55% in lamina VI and ~40% in lamina V, and gradually decreasing in lamina VIII, X and VII (~28%, ~14% and ~12%, respectively) (**Figure 2c-d**). No co-localizations were detected in lamina I, II and IX (**Figure 2c-d**). In contrast, the percentage of pS32-cFos/GFP co-expressing cells reached ~26% and ~19% in lamina IV and III, respectively (**Figure 2c-d**). These findings indicate that d-amphetamine induces pS32-cFos expression preferentially in glycinergic inhibitory neurons.

Finally, the distribution of pS32-cFos expression was analyzed in VGluT2-expressing excitatory neurons (**Figure 2e-f**). To do so, we generated *VGlut2-Ribotag* mice, which express the ribosomal protein Rpl22 tagged with hemagglutinin (HA) exclusively in glutamatergic VGluT2 neurons. As shown in Figure 2f, percentages of pS32-cFos/HA co-expressing neurons were high in all the laminae in which d-amphetamine increased pS32-cFos expression (~40% in lamina VII and VIII; ~33% in lamina X; ~28% in lamina VI and ~20% in lamina V) (**Figure 2e-f**). Altogether, our analyses show that d-amphetamine increases pS32-cFos expression in both inhibitory and excitatory neurons expressing GlyT2/Gad67 and VGluT2, respectively.

Distribution of d-amphetamine-induced pS32-cFos immunoreactive cells among neurons identified by calcium-binding proteins

To further characterize the molecular identity of activated pS32-cFos-positive neurons in the lumbar spinal cord in response to d-amphetamine, we analyzed the percentage

of co-localization between pS32-cFos-immunoreactive neurons and those expressing calcium-binding proteins (CBP), calbindin-D28k (CB), calretinin (CR), and parvalbumin (PV) (**Figure 2g-l**). Overall, our analysis revealed low or no co-localization between pS32-cFos and CB in lamina V, VI and VII (~1%) and lamina VIII and IX (0) (**Figure 2g-h**). Similarly, pS32-cFos/CR-positive cells represented ~2% of the total pS32-cFos in the lamina V and VIII, and only ~1% in lamina VI and VII (**Figure 2i-j**). The highest percentages of co-localization were found between pS32-cFos and PV in lamina V (~7%) and VI (~4%), corresponding to 8 and 13 pS32-cFos/PV-positive cells among the 108 and 283 pS32-cFos-immunoreative cells (**Figure 2k-l, Table 3**). Strikingly, although d-amphetamine failed to significantly increase pS32-cFos in lamina II (see **Figure 1**), our analysis revealed that a high percentage of the few pS32-cFos-positive neurons co-expressed CR (~31%) and to a lesser extent PV (~9%) and CB (~7%) (**Figure 2i-j**). Together, these results indicate that pS32-cFos expression induced by d-amphetamine does not preferentially occur in calcium-binding proteins-expressing cells in the lumbar spinal cord.

Reactivation of d-amphetamine-tagged neurons following d-amphetamine re-exposure in the lumbar spinal cord

We sought to determine whether lumbar spinal cord neuronal activation evoked by a single exposure of d-amphetamine was more prone to be re-activated by a second administration of d-amphetamine. *cFos-CreERT2-Trap* mice were injected with saline or d-amphetamine (10 mg/kg) prior to the administration of 4-OHT (day 1), triggering the cFos driven expression of GFP in activated neurons, and re-injected with d-amphetamine a week after (day 7). No significant changes were detected in laminae I ($t_7 = 1.758$, $p = 0.1222$), II ($t_7 = 0.8013$, $p = 0.4493$), VIII ($t_7 = 1.610$, $p = 0.1514$) and

IX (t_7 = 0.1584, p = 0.8786) (**Figure 3a-b**). In contrast, d-amphetamine-treated mice on day 1 displayed a higher number of GFP-tagged neurons compared to saline-injected mice in lamina III (t_7 = 3.606, p = 0.0087), IV (t_7 = 3.382, p = 0.0117), V (t_7 = 2.540, p = 0.0387), VI (t_7 = 2.683, p = 0.0314), VII (t_7 = 2.949, p = 0.0214) and X (t_7 = 3.085, p = 0.0177) (**Figure 3a-b**). Interestingly, the analysis of the percentage of co-localization between pS32-cFos-immunoreactive neurons induced by the administration of d-amphetamine on day 7 and those expressing GFP in response to a first injection of d-amphetamine revealed that about one-third of the d-amphetamine-tagged neurons were re-activated following d-amphetamine re-exposure (~43-44% in lamina III and X; ~37-38% in lamina VI and IV; ~33% in lamina V and ~29% in lamina VII) (**Figure 3c-d**).

Various psychostimulant drugs increase pS32-cFos expression in lumbar spinal cord

We next investigated whether two psychostimulant drugs, cocaine and methylphenidate, could trigger the expression of pS32-cFos in the lumbar spinal cord. Similarly to d-amphetamine, a single administration of cocaine (15 mg/kg) or methylphenidate (15 mg/kg) increased pS32-cFos expression in lumbar spinal cord at 90 min (**Figure 4**). All tested psychostimulant drugs tested shared the property of increasing the number of pS32-cFos-positive neurons in lamina III (cocaine t_4 = 5.367, p = 0.0058; methylphenidate t_5 = 4.283, p = 0.0078), V (cocaine t_4 = 3.286, p = 0.0303; methylphenidate t_5 = 4.048, p = 0.0098), VI (cocaine t_4 = 7.141, p = 0.0020; methylphenidate t_5 = 3.901, p = 0.0114), VII (cocaine t_4 = 7.906, p = 0.0014; methylphenidate t_5 = 5.615, p = 0.0025) and VIII (cocaine t_4 = 2.286, p = 0.0843; methylphenidate t_5 = 2.46, p = 0.0572) (**Figures 1b and 4a-d**). On the other hand, the

increased pS32-cFos expression in lamina I was only observed after the administration of cocaine (t_4 = 3.051, p = 0.038; methylphenidate t_5 = 0.9555, p = 0.3832) (**Figure 4a-b**), while the increase in lamina X was only produced by methylphenidate (cocaine t_4 = 0.3592, p = 0.7376; methylphenidate t_5 = 4.792, p = 0.0049) (**Figure 4c-d**). No significant changes were detected in laminae II (cocaine t_4 = 1.908, p = 0.1290; methylphenidate t_5 = 0.4085, p = 0.6998) and IV (t_4 = 1.835, p = 0.1404; methylphenidate t_5 = 1.832, p = 0.1265)

At the doses used here, acute d-amphetamine, cocaine and methylphenidate cause strong locomotor responses (Gangarossa et al., 2019; Valjent et al., 2010). To determine whether the induction of pS32-cFos in the lumbar spinal cord was the sole consequence of a generalized hyperlocomotion, we analyzed pS32-cFos expression in response to morphine, an agonist of μ, δ and κ opioid receptors, and dizocilpine (MK801), a noncompetitive NMDA receptor blocker. As shown in Figure 5, acute administration of morphine (5 mg/kg) or dizocilpine (0.3 mg/kg) administered at doses capable to enhance locomotor activity (Puighermanal et al., 2020; Valjent et al., 2010) failed to trigger pS32-cFos expression in the lumbar spinal cord (lamina I: $F_{2, 12}$ = 0.6433, p = 0.5428; lamina II: $F_{2, 12}$ = 1.571, p = 0.2477; lamina III: $F_{2, 12}$ = 0.1978, p = 0.8232; lamina IV: $F_{2, 12}$ = 0.9372, p = 0.4186; lamina V: $F_{2, 12}$ = 1.397, p = 0.2848; lamina VI: $F_{2, 12}$ = 0.8756, p = 0.4416; lamina VII: $F_{2, 12}$ = 3.906, p = 0.0494; lamina VIII: $F_{2, 12}$ = 3.21, p = 0.0764; lamina X: $F_{2, 12}$ = 0.6678, p = 0.5309) (**Figure 5a-b**). Together, these results suggest that the induction of pS32-cFos in response to psychostimulant is not a direct consequence of hyperlocomotion but rather of a specific effect of this class of drugs.

Regulation of pS32-cFos expression in lumbar spinal cord by monoamine reuptake inhibitors

D-amphetamine, cocaine, and methylphenidate increase the extracellular concentration of DA, norepinephrine, and serotonin (Torres et al., 2003). Therefore, we investigated whether increasing the extracellular concentration of these monoamines was sufficient to trigger pS32-cFos expression in lumbar spinal cord. We compared pS32-cFos expression in C57BL/6 mice administered with d-amphetamine or different monoamine reuptake inhibitors 90 min after injection (lamina I: $F_{3, 11}$ = 1.143, p = 0.3747; lamina II: $F_{3, 11}$ = 1.908, p = 0.1867; lamina III: $F_{3, 11}$ = 6.276, p = 0.0097; lamina IV: $F_{3, 11}$ = 5.729, p = 0.0128; lamina V: $F_{3, 11}$ = 16.07, p = 0.0002; lamina VI: $F_{3, 11}$ = 19.42, p = 0.0001; lamina VII: $F_{3, 11}$ = 7.06, p = 0.0065; lamina VIII: $F_{3, 11}$ = 6.325, p = 0.0094; lamina X: $F_{3, 11}$ = 4.131, p = 0.0345) (**Figure 6**). The administration of mixed norepinephrine and serotonin reuptake inhibitors, desipramine (15 mg/kg) or imipramine (10 mg/kg), failed to increase pS32-cFos expression in lumbar spinal cord (**Figure 6a-b**). In contrast, the selective DA reuptake inhibitor, GBR12783 (15 mg/kg), injected a dose increasing locomotion (Valjent et al., 2010) triggered a pattern of pS32-cFos expression that resembled the one induced by psychostimulant drugs, thus indicating that blockade of DA reuptake is sufficient to increase pS32-cFos expression in lumbar spinal cord (**Figure 6a-b**).

Discussion

The present study unveils that a single administration of d-amphetamine, at a dose inducing motor activity and stereotypies (Gangarossa et al., 2019), activates pS32-cFos-expressing neurons in the dorsal and ventral lumbar spinal cord. We also demonstrate that d-amphetamine-induced pS32-cFos occurs in both excitatory and inhibitory interneurons distributed in various laminae associated with sensory processing and motor function. In contrast, no significant changes in pS32-cFos expression were detected in motor neurons or in superficial laminae of the dorsal spinal cord. Finally, we provide evidence that GBR12783, a selective DA reuptake inhibitor, is sufficient to trigger a similar pattern of increased pS32-cFos expression to those induced by all dopaminomimetic drugs.

In rodents, a single administration of d-amphetamine induces a broad repertoire of motor behaviors ranging from increased locomotion (from 2 to 5 mg/kg) to repetitive/stereotyped motor sequences (above 5 mg/kg) (Crittenden et al., 2014; Mansouri-Guilani et al., 2019; Valjent et al., 2010; Yates et al., 2007). Our results indicate that the latter are correlated with an increased expression of pS32-cFos in neurons in the ventral horn of the spinal cord, a spinal region harboring neural circuits dedicated to execution and generation of rhythmic motor behaviors (Grillner and El Manira, 2020). Redex laminae delineation-based analysis revealed that d-amphetamine failed to increase pS32-cFos expression in lamina IX where motor neurons are located. Conversely, pS32-cFos-immunolabeled neurons were observed in laminae VII and VIII suggesting that d-amphetamine might preferentially activate a subpopulation of neurons of the locomotor central pattern generator network (Grillner and El Manira, 2020). The high percentage of pS32-cFos/VGluT2 and pS32-

cFos/GlyT2-positive neurons in the aforementioned layers indicates that d-amphetamine-induced pS32-cFos may occur in a fraction of both excitatory and inhibitory interneurons of the locomotor central pattern generator network (Grillner and El Manira, 2020). The analysis of the distribution of pS32-cFos among the CBP-expressing interneurons constituted a first attempt to clarify the molecular identity of pS32-cFos-positive cells (Alvarez et al., 2005; Floyd et al., 2018; Lu et al., 2015). Thus, the lack of pS32-cFos/CB-positive cells along the ventral-gray-white matter border in laminae VII and VIII indicates that d-amphetamine does not activate Renshaw cells, which are known to mediate recurrent inhibition of motor neurons (Alvarez et al., 2005). Moreover, the negligible percentage of pS32-cFos found in CB/PV-positive neurons detected in lamina VII also suggests that d-amphetamine-activated cells do not recruit V1-derived interneurons (Alvarez et al., 2005). Given the motor patterns induced by d-amphetamine, future experiments will be necessary to determine whether increased pS32-cFos expression occurs in excitatory V2 and inhibitory V0 interneurons, both controlling the left-right coordination of limbs.

D-amphetamine induced a prominent increase of pS32-cFos in excitatory ($VGluT2^+$) and inhibitory ($GlyT2^+$ and to a lesser extent $Gad67^+$) neurons of laminae V and VI of the SC dorsal horn. This spinal region contains premotor neurons also designated as motor synergy encoder neurons (Levine et al., 2014; Osseward and Pfaff, 2019). These neurons, which derive from discrete dorsal and ventral progenitor domains (Lai et al., 2016), control the activation of spatially segregated pools of motor neurons, thereby participating in the fine-tuning of complex coordinated motor actions (Levine et al., 2014). They also integrate convergent proprioceptive and corticospinal signals conveying sensory feedbacks necessary to adjust motor

behaviors (Hilde et al., 2016; Osseward and Pfaff, 2019). Thus, by exacerbating the activity of motor synergy encoder neurons through a mechanism that remains to be established, psychostimulants may hijack the aforementioned functions altering somatosensory processing and therefore favoring patterned motor activities as well as in-place stereotyped motor sequences.

DA arising from midbrain and forebrain nuclei modulates the activity of neural networks controlling motor behaviors (Grillner and El Manira, 2020). Indeed, ascending and descending midbrain DA systems have been characterized, all serving distinct but complementary roles in the regulation of movement. For instance, midbrain (A9 and A10 nuclei) DA neurons are known to regulate motor planning and execution indirectly through ascending projections to basal ganglia circuits (Grillner and El Manira, 2020). An increased extracellular concentration of DA within these circuits has been causally associated with the ability of psychostimulant drugs to promote motor hyper-responsiveness as well as neuronal activation (Graybiel et al., 1990; Moratalla et al., 1993). Interestingly, increasing evidence suggests that DA might also indirectly control locomotion through A9/A10 and A13 descending DA pathways which innervate the two major brainstem excitatory nuclei of mesencephalic locomotor region, the pedunculopontine nucleus and the cuneiform nucleus (Ryczko et al., 2016; Ryczko and Dubuc, 2017; Sharma et al., 2018). Finally, recent works indicate that opto-activation of the descending DA pathway originating from A11 nuclei known to modulate spinal networks involved in the control of rhythmic movements (Han et al., 2007; Pappas et al., 2008; Sharples et al., 2020; Sharples et al., 2014) is sufficient to increase both locomotion and in-place activity (Koblinger et al., 2018). Surprisingly, no evidence has yet indicated that this pathway might

participate in the regulation of motor behaviors induced by psychostimulants. Though addressing this question was not the purpose of the present work, our findings raise the question of the contribution of descending DA neurons in the increase of spinal cFos expression by psychostimulants. Thus, although the widespread distribution of DA projections in lumbar spinal cord might at least in part explain the pattern of cFos induction, functional features of A11 DA neurons question the mechanisms by which psychostimulants would promote the increase of spinal DA concentration. Indeed, spinal DA projections arising from A11 nucleus lack the dopamine transporter (Koblinger et al., 2014; Pappas et al., 2008), suggesting that the DA-dependent neuronal in the spinal cord may not result from the direct action of psychostimulants onto A11 TH-positive terminals but rather from a network effect.

Beside their ability to increase DA extracellular levels, psychostimulants are potent releasers of other biogenic amines including norepinephrine (Gatley et al., 1996; Kuczenski and Segal, 1997) that also contributes to the regulation of psychostimulant-induced motor hyperactivity (Drouin et al., 2002). Interestingly, such regulation occurs mainly through the stimulation of alpha1-adrenergic receptors, which are highly expressed in the spinal cord (Day et al., 1997; Drouin et al., 2002). Whether pontine A7 and A6 (locus coeruleus) descending norepinephrine neurons (Bruinstroop et al., 2012), that co-express DA, contribute to the regulation of cFos expression induced by psychostimulants through this class of adrenergic receptors will require future investigation.

Over the last decade, compelling evidence indicate that cFos-expressing neurons activated by drugs of abuse define region-specific neuronal ensembles which are causally linked to both conditioned-drug effects and drug-seeking behavior (Cruz et

al., 2013). Indeed, selective inactivation of cocaine-activated neurons in the nucleus accumbens has been shown to prevent context-dependent locomotor sensitization to cocaine and context-induced reinstatement of cocaine seeking (Cruz et al., 2014; Koya et al., 2009). Moreover, distinct cFos-expressing neuronal ensembles in the ventromedial prefrontal cortex encode cocaine self-administration, extinction or cocaine seeking (Kane et al., 2021; Warren et al., 2019) as well as context-induced relapse to heroin (Bossert et al., 2011). Further work will be needed to establish whether cFos-expressing spinal neurons identified in laminae hosting locomotor central pattern generator network and motor synergy encoder neurons define selective neuronal ensembles and whether a dysfunction of these ensembles is causally linked to the enduring psychomotor tremor and proprioceptive deficits developed in response to psychostimulants exposure (Downey et al., 2017).

Conflict of interest

The authors declare no conflict of interest.

Acknowledgments

The authors thank Jean-Antoine Girault and Giuseppe Gangarossa for critical reading of the manuscript and for their insightful comments. We thank the RAM-iExplore facility for their involvement in the maintenance and breeding of the colonies. This work was supported by Inserm, Fondation pour la Recherche Médicale (EQU202203014705), Agence National de la Recherche (DISCOMMODE, ANR-21-CE37-0013; FrontoFat, ANR-20-CE14-0020; ANR SubDOPA, ANR-21-CE16-0028) (E.V.). Laura Cutando was supported by the post-doctoral Labex EpiGenMed fellowship («Investissements d'avenir» ANR-10-LABX-12-01). Laia Castell was supported by the pre-doctoral Labex EpiGenMed («Investissements d'avenir» ANR-10-LABX-12-01). Coline Rulhe is supported by a fellowship from the French Ministry of Higher Education and Research.

References

Allen, W.E., DeNardo, L.A., Chen, M.Z., Liu, C.D., Loh, K.M., Fenno, L.E., Ramakrishnan, C., Deisseroth, K., and Luo, L. (2017). Thirst-associated preoptic neurons encode an aversive motivational drive. Science *357*, 1149-1155.10.1126/science.aan6747.

Alvarez, F.J., Jonas, P.C., Sapir, T., Hartley, R., Berrocal, M.C., Geiman, E.J., Todd, A.J., and Goulding, M. (2005). Postnatal phenotype and localization of spinal cord V1 derived interneurons. J Comp Neurol *493*, 177-192.10.1002/cne.20711.

Berke, J.D., Paletzki, R.F., Aronson, G.J., Hyman, S.E., and Gerfen, C.R. (1998). A complex program of striatal gene expression induced by dopaminergic stimulation. J Neurosci *18*, 5301-5310.

Bertran-Gonzalez, J., Bosch, C., Maroteaux, M., Matamales, M., Herve, D., Valjent, E., and Girault, J.A. (2008). Opposing patterns of signaling activation in dopamine D1 and D2 receptor-expressing striatal neurons in response to cocaine and haloperidol. J Neurosci *28*, 5671-5685.10.1523/JNEUROSCI.1039-08.2008.

Bossert, J.M., Stern, A.L., Theberge, F.R., Cifani, C., Koya, E., Hope, B.T., and Shaham, Y. (2011). Ventral medial prefrontal cortex neuronal ensembles mediate context-induced relapse to heroin. Nat Neurosci *14*, 420-422.10.1038/nn.2758.

Bruinstroop, E., Cano, G., Vanderhorst, V.G., Cavalcante, J.C., Wirth, J., Sena-Esteves, M., and Saper, C.B. (2012). Spinal projections of the A5, A6 (locus coeruleus), and A7 noradrenergic cell groups in rats. J Comp Neurol *520*, 1985-2001.10.1002/cne.23024.

Canales, J.J., and Graybiel, A.M. (2000). Patterns of gene expression and behavior induced by chronic dopamine treatments. Ann Neurol *47*, S53-59.

Crittenden, J.R., Lacey, C.J., Lee, T., Bowden, H.A., and Graybiel, A.M. (2014). Severe drug-induced repetitive behaviors and striatal overexpression of VAChT in ChAT-ChR2-EYFP BAC transgenic mice. Front Neural Circuits *8*, 57.10.3389/fncir.2014.00057.

Cruz, F.C., Babin, K.R., Leao, R.M., Goldart, E.M., Bossert, J.M., Shaham, Y., and Hope, B.T. (2014). Role of nucleus accumbens shell neuronal ensembles in context-induced reinstatement of cocaine-seeking. J Neurosci *34*, 7437-7446.10.1523/JNEUROSCI.0238-14.2014.

Cruz, F.C., Koya, E., Guez-Barber, D.H., Bossert, J.M., Lupica, C.R., Shaham, Y., and Hope, B.T. (2013). New technologies for examining the role of neuronal ensembles in drug addiction and fear. Nat Rev Neurosci *14*, 743-754.10.1038/nrn3597.

Day, H.E., Campeau, S., Watson, S.J., Jr., and Akil, H. (1997). Distribution of alpha 1a-, alpha 1b- and alpha 1d-adrenergic receptor mRNA in the rat brain and spinal cord. J Chem Neuroanat *13*, 115-139.10.1016/s0891-0618(97)00042-2.

Downey, L.A., Tysse, B., Ford, T.C., Samuels, A.C., Wilson, R.P., and Parrott, A.C. (2017). Psychomotor Tremor and Proprioceptive Control Problems in Current and Former Stimulant Drug Users: An Accelerometer Study of Heavy Users of Amphetamine, MDMA, and Other Recreational Stimulants. J Clin Pharmacol *57*, 1330-1337.10.1002/jcph.925.

Drouin, C., Blanc, G., Villegier, A.S., Glowinski, J., and Tassin, J.P. (2002). Critical role of alpha1-adrenergic receptors in acute and sensitized locomotor effects of D-amphetamine, cocaine, and GBR 12783: influence of preexposure conditions and pharmacological characteristics. Synapse *43*, 51-61.10.1002/syn.10023.

Floyd, T.L., Dai, Y., and Ladle, D.R. (2018). Characterization of calbindin D28k expressing interneurons in the ventral horn of the mouse spinal cord. Dev Dyn *247*, 185-193.10.1002/dvdy.24601.

Gangarossa, G., Castell, L., Castro, L., Tarot, P., Veyrunes, F., Vincent, P., Bertaso, F., and Valjent, E. (2019). Contrasting patterns of ERK activation in the tail of the striatum in response to aversive and rewarding signals. J Neurochem *151*, 204-226.10.1111/jnc.14804.

Gatley, S.J., Pan, D., Chen, R., Chaturvedi, G., and Ding, Y.S. (1996). Affinities of methylphenidate derivatives for dopamine, norepinephrine and serotonin transporters. Life Sci *58*, 231-239.10.1016/0024-3205(96)00052-5.

Gaytan, O., Swann, A., and Dafny, N. (1998). Time-dependent differences in the rat's motor response to amphetamine. Pharmacology, biochemistry, and behavior *59*, 459-467.10.1016/s0091-3057(97)00438-3.

Geisler, S., Marinelli, M., Degarmo, B., Becker, M.L., Freiman, A.J., Beales, M., Meredith, G.E., and Zahm, D.S. (2008). Prominent activation of brainstem and pallidal afferents of the ventral tegmental area by cocaine. Neuropsychopharmacology *33*, 2688-2700.10.1038/sj.npp.1301650.

Graybiel, A.M., Moratalla, R., and Robertson, H.A. (1990). Amphetamine and cocaine induce drug-specific activation of the c-fos gene in striosome-matrix compartments and limbic subdivisions of the striatum. Proc Natl Acad Sci U S A *87*, 6912-6916.10.1073/pnas.87.17.6912.

Grillner, S., and El Manira, A. (2020). Current Principles of Motor Control, with Special Reference to Vertebrate Locomotion. Physiological reviews *100*, 271-320.10.1152/physrev.00015.2019.

Han, P., Nakanishi, S.T., Tran, M.A., and Whelan, P.J. (2007). Dopaminergic modulation of spinal neuronal excitability. J Neurosci *27*, 13192-13204.10.1523/JNEUROSCI.1279-07.2007.

Hilde, K.L., Levine, A.J., Hinckley, C.A., Hayashi, M., Montgomery, J.M., Gullo, M., Driscoll, S.P., Grosschedl, R., Kohwi, Y., Kohwi-Shigematsu, T.*, et al.* (2016). Satb2 Is Required for the Development of a Spinal Exteroceptive Microcircuit that Modulates Limb Position. Neuron *91*, 763-776.10.1016/j.neuron.2016.07.014.

Kane, L., Venniro, M., Quintana-Feliciano, R., Madangopal, R., Rubio, F.J., Bossert, J.M., Caprioli, D., Shaham, Y., Hope, B.T., and Warren, B.L. (2021). Fos-expressing neuronal ensemble in rat ventromedial prefrontal cortex encodes cocaine seeking but not food seeking in rats. Addict Biol *26*, e12943.10.1111/adb.12943.

Koblinger, K., Fuzesi, T., Ejdrygiewicz, J., Krajacic, A., Bains, J.S., and Whelan, P.J. (2014). Characterization of A11 neurons projecting to the spinal cord of mice. PLoS One *9*, e109636.10.1371/journal.pone.0109636.

Koblinger, K., Jean-Xavier, C., Sharma, S., Fuzesi, T., Young, L., Eaton, S.E.A., Kwok, C.H.T., Bains, J.S., and Whelan, P.J. (2018). Optogenetic Activation of A11 Region Increases Motor Activity. Front Neural Circuits *12*, 86.10.3389/fncir.2018.00086.

Koya, E., Golden, S.A., Harvey, B.K., Guez-Barber, D.H., Berkow, A., Simmons, D.E., Bossert, J.M., Nair, S.G., Uejima, J.L., Marin, M.T.*, et al.* (2009). Targeted disruption of cocaine-activated nucleus accumbens neurons prevents context-specific sensitization. Nat Neurosci *12*, 1069-1073.10.1038/nn.2364.

Kuczenski, R., and Segal, D.S. (1997). Effects of methylphenidate on extracellular dopamine, serotonin, and norepinephrine: comparison with amphetamine. J Neurochem *68*, 2032-2037.10.1046/j.1471-4159.1997.68052032.x.

Lai, H.C., Seal, R.P., and Johnson, J.E. (2016). Making sense out of spinal cord somatosensory development. Development *143*, 3434-3448.10.1242/dev.139592.

Levine, A.J., Hinckley, C.A., Hilde, K.L., Driscoll, S.P., Poon, T.H., Montgomery, J.M., and Pfaff, S.L. (2014). Identification of a cellular node for motor control pathways. Nat Neurosci *17*, 586-593.10.1038/nn.3675.

Liu, J., Krautzberger, A.M., Sui, S.H., Hofmann, O.M., Chen, Y., Baetscher, M., Grgic, I., Kumar, S., Humphreys, B.D., Hide, W.A.*, et al.* (2014). Cell-specific translational profiling in acute kidney injury. J Clin Invest *124*, 1242-1254.10.1172/JCI72126.

Lu, D.C., Niu, T., and Alaynick, W.A. (2015). Molecular and cellular development of spinal cord locomotor circuitry. Front Mol Neurosci *8*, 25.10.3389/fnmol.2015.00025.

Mansouri-Guilani, N., Bernard, V., Vigneault, E., Vialou, V., Daumas, S., El Mestikawy, S., and Gangarossa, G. (2019). VGLUT3 gates psychomotor effects induced by amphetamine. J Neurochem *148*, 779-795.10.1111/jnc.14644.

Moratalla, R., Vickers, E.A., Robertson, H.A., Cochran, B.H., and Graybiel, A.M. (1993). Coordinate expression of c-fos and jun B is induced in the rat striatum by cocaine. J Neurosci *13*, 423-433.

Osseward, P.J., 2nd, and Pfaff, S.L. (2019). Cell type and circuit modules in the spinal cord. Curr Opin Neurobiol *56*, 175-184.10.1016/j.conb.2019.03.003.

Pappas, S.S., Behrouz, B., Janis, K.L., Goudreau, J.L., and Lookingland, K.J. (2008). Lack of D2 receptor mediated regulation of dopamine synthesis in A11 diencephalospinal neurons in male and female mice. Brain Res *1214*, 1-10.10.1016/j.brainres.2008.03.010.

Puighermanal, E., Biever, A., Espallergues, J., Gangarossa, G., De Bundel, D., and Valjent, E. (2015). drd2-cre:ribotag mouse line unravels the possible diversity of dopamine d2 receptor-expressing cells of the dorsal mouse hippocampus. Hippocampus *25*, 858-875.10.1002/hipo.22408.

Puighermanal, E., Castell, L., Esteve-Codina, A., Melser, S., Kaganovsky, K., Zussy, C., Boubaker-Vitre, J., Gut, M., Rialle, S., Kellendonk, C.*, et al.* (2020). Functional and molecular heterogeneity of D2R neurons along dorsal ventral axis in the striatum. Nat Commun *11*, 1957.10.1038/s41467-020-15716-9.

Ryczko, D., Cone, J.J., Alpert, M.H., Goetz, L., Auclair, F., Dube, C., Parent, M., Roitman, M.F., Alford, S., and Dubuc, R. (2016). A descending dopamine pathway conserved from basal vertebrates to mammals. Proc Natl Acad Sci U S A *113*, E2440-2449.10.1073/pnas.1600684113.

Ryczko, D., and Dubuc, R. (2017). Dopamine and the Brainstem Locomotor Networks: From Lamprey to Human. Front Neurosci *11*, 295.10.3389/fnins.2017.00295.

Sanz, E., Yang, L., Su, T., Morris, D.R., McKnight, G.S., and Amieux, P.S. (2009). Cell-type-specific isolation of ribosome-associated mRNA from complex tissues. Proc Natl Acad Sci U S A *106*, 13939-13944.10.1073/pnas.0907143106.

Sasaki, T., Kojima, H., Kishimoto, R., Ikeda, A., Kunimoto, H., and Nakajima, K. (2006). Spatiotemporal regulation of c-Fos by ERK5 and the E3 ubiquitin ligase UBR1, and its biological role. Mol Cell *24*, 63-75.10.1016/j.molcel.2006.08.005.

Sharma, S., Kim, L.H., Mayr, K.A., Elliott, D.A., and Whelan, P.J. (2018). Parallel descending dopaminergic connectivity of A13 cells to the brainstem locomotor centers. Sci Rep *8*, 7972.10.1038/s41598-018-25908-5.

Sharples, S.A., Burma, N.E., Borowska-Fielding, J., Kwok, C.H.T., Eaton, S.E.A., Baker, G.B., Jean-Xavier, C., Zhang, Y., Trang, T., and Whelan, P.J. (2020). A dynamic role for dopamine receptors in the control of mammalian spinal networks. Sci Rep *10*, 16429.10.1038/s41598-020-73230-w.

Sharples, S.A., Koblinger, K., Humphreys, J.M., and Whelan, P.J. (2014). Dopamine: a parallel pathway for the modulation of spinal locomotor networks. Front Neural Circuits *8*, 55.10.3389/fncir.2014.00055.

Torres, G.E., Gainetdinov, R.R., and Caron, M.G. (2003). Plasma membrane monoamine transporters: structure, regulation and function. Nat Rev Neurosci *4*, 13-25.10.1038/nrn1008.

Valjent, E., Bertran-Gonzalez, J., Aubier, B., Greengard, P., Herve, D., and Girault, J.A. (2010). Mechanisms of locomotor sensitization to drugs of abuse in a two-injection protocol. Neuropsychopharmacology *35*, 401-415.10.1038/npp.2009.143.

Warren, B.L., Kane, L., Venniro, M., Selvam, P., Quintana-Feliciano, R., Mendoza, M.P., Madangopal, R., Komer, L., Whitaker, L.R., Rubio, F.J.*, et al.* (2019). Separate vmPFC Ensembles Control Cocaine Self-Administration Versus Extinction in Rats. J Neurosci *39*, 7394-7407.10.1523/JNEUROSCI.0918-19.2019.

Yates, J.W., Meij, J.T., Sullivan, J.R., Richtand, N.M., and Yu, L. (2007). Bimodal effect of amphetamine on motor behaviors in C57BL/6 mice. Neurosci Lett *427*, 66-70.10.1016/j.neulet.2007.09.011.

Ztaou, S., Oh, S.J., Tepler, S., Fleury, S., Matamales, M., Bertran-Gonzalez, J., Chuhma, N., and Rayport, S. (2021). Single Dose of Amphetamine Induces Delayed Subregional Attenuation of Cholinergic Interneuron Activity in the Striatum. eNeuro *8*.10.1523/ENEURO.0196-21.2021.

Figure legends

Figure 1: Induction of pS32-cFos expression in lumbar spinal cord by d-amphetamine. a pS32-cFos immunoreactivity in the lumbar spinal cord of C57BL/6 mice after saline or d-amphetamine (d-amph) (10 mg/kg) administration. Scale bar, 200 µm. **b** Quantification of pS32-cFos-immunoreactive neurons in the distinct laminae of the lumbar spinal cord of C57BL/6 mice treated with saline (n = 3 mice) or d-amphetamine and perfused 30 (n = 3 mice), 60 (n = 3 mice), 90 (n = 3 mice) and 120 min (n = 3 mice) after injection. Data analyzed using one-way ANOVA followed by Šidák's multiple comparisons test. All data are presented as means ± sem. * $p < 0.05$, ** $p < 0.01$ saline vs. d-amphetamine.

Figure 2: Molecular identification of pS32-cFos-positive neurons in lumbar spinal cord in response to d-amphetamine. a, **c**, **e** Double immunofluorescence for pS32-cFos (red) and GFP (green) (**a**, **c**), and HA (green) (**e**) in the lumbar spinal cord of *Gad67-eGFP* (n = 3 mice) (**a**), *GlyT2-eGFP* (n = 4 mice) (**c**) and *VGlut2-Ribotag* (n = 3 mice) (**e**) mice treated with d-amphetamine (10 mg/kg). High magnification images of the areas delineated by the yellow stippled rectangles. White arrowheads indicate pS32-cFos/GFP- or pS32-cFos/HA-positive neurons. Scale bars, 200 µm (left panels), 100 µm (right panels). **b**, **d**, **f** Histograms showing the co-expression of pS32-cFos/GFP (**b**, **d**) and pS32-cFos/HA (**e**) as percentage of pS32-cFos-immunoreactive neurons in the distinct laminae of the lumbar spinal cord of *Gad67-eGFP* (**b**), *GlyT2-eGFP* (**d**) and *VGlut2-Ribotag* (**e**) treated with d-amphetamine and perfused 90 min after injection. **g**, **i**, **k** Double immunofluorescence for pS32-cFos (red) and calbindin-D28k (green, CB) (**g**), calretinin (green, CR) (**i**), and parvalbumin (green, PV) (**k**) in the lumbar spinal cord of C57BL/6 mice (n = 5-7) treated with d-amphetamine (10

mg/kg). High magnification images of the areas delineated by the yellow stippled rectangles. White arrowheads indicate pS32-cFos-positive neurons co-expressing CB, CR or PV. Scale bars, 200 µm (left panels), 100 µm (right panels). **h**, **j**, **l** Histograms showing the co-expression of pS32-cFos/CB (**h**), pS32-cFos/CR (**j**) and pS32-cFos/PV (**l**) as percentage of pS32-cFos-immunoreactive neurons in the distinct laminae of the lumbar spinal cord of C57BL/6 mice treated with d-amphetamine and perfused 90 min after injection. Numbers of pS32-cFos-positive neurons counted are reported in Table 3.

Figure 3: Reactivation of d-amphetamine-tagged neurons following d-amphetamine re-exposure in the lumbar spinal cord. a GFP fluorescence in the lumbar spinal cord of *cFos-CreERT2-Trap* mice treated with saline or d-amphetamine (10 mg/kg) on day 1. Scale bar, 200 µm. **b** Quantification of the number of activity-tagged neurons (GFP^+) in mice treated with saline (n = 4 mice) or d-amphetamine (n = 5 mice) on day 1. Data analyzed using Student *t*-test two-sided. All data are presented as means ± sem. * $p < 0.05$, ** $p < 0.01$ saline vs. d-amphetamine **c** GFP fluorescence (green) and pS32-cFos immunoreactivity (red) in the lumbar spinal cord of a *cFos-CreERT2-Trap* mouse treated with d-amphetamine on day 1 and 7. Scale bar, 200 µm (left panels), 30 µm (right panels). **d** Histograms showing the co-expression of pS32-cFos/GFP as percentage of GFP-immunoreactive neurons in the distinct laminae of the lumbar spinal cord of *cFos-CreERT2-Trap* mice treated with d-amphetamine on day 1 and 7 and perfused 90 min after the administration on day 7. Numbers of GFP-positive neurons counted are reported in Table 3.

Figure 4: Cocaine and methylphenidate increase pS32-cFos expression in lumbar spinal cord. a, **c** pS32-cFos immunoreactivity in the lumbar spinal cord of C57BL/6 mice 90 min after saline or cocaine (15 mg/kg) (**a**) and methylphenidate (15 mg/kg) (**c**) administration. Scale bar, 200 µm. **b**, **d** Quantification of pS32-cFos-immunoreactive neurons in the distinct laminae of the lumbar spinal cord of C57BL/6 mice treated with saline (n = 3 mice) and cocaine (n = 3 mice) (**b**) or (n = 3 mice) and methylphenidate (n = 4 mice) (**d**), and perfused 90 min after injection. Data analyzed using Student *t*-test two-sided. All data are presented as means ± sem. * $p < 0.05$, ** $p < 0.01$ saline vs. drugs.

Figure 5: Morphine and dizocilpine fail to induce pS32-cFos in lumbar spinal cord. a pS32-cFos immunoreactivity in the lumbar spinal cord of C57BL/6 mice 90 min after saline, morphine (5 mg/kg) or dizocilpine (0.3 mg/kg) administration. Scale bar, 200 µm. **b** Quantification of pS32-cFos-immunoreactive neurons in the distinct laminae of the lumbar spinal cord of C57BL/6 mice treated with saline (n = 5 mice), morphine (n = 4 mice) or dizocilpine (n = 6 mice) and perfused 90 min after injection. Data analyzed using one-way ANOVA followed by Šidák's multiple comparisons test. All data are presented as means ± sem.

Figure 6: Dopamine reuptake inhibitor increases pS32-cFos expression in lumbar spinal cord. a pS32-cFos immunoreactivity in the lumbar spinal cord of C57BL/6 mice 90 min after d-amphetamine (10 mg/kg), imipramine (10 mg/kg), desipramine (15 mg/kg) or GBR12783 (15 mg/kg) administration. Scale bar, 200 µm. **b** Quantification of pS32-cFos-immunoreactive neurons in the distinct laminae of the lumbar spinal cord of C57BL/6 mice treated with d-amphetamine (n = 5 mice),

imipramine (n = 3 mice), desipramine (n = 3) or GBR12783 (n = 4 mice) and perfused 90 min after injection. Dashed lines represent the number of cells in saline-treated mice. Data analyzed using one-way ANOVA followed by Šidák's multiple comparisons test. All data are presented as means ± sem. * $p < 0.05$, ** $p < 0.01$ d-amphetamine vs. drugs. # $p < 0.05$, ## $p < 0.01$ GBR12783 vs. drugs.

List of Abbreviations

4-OHT: 4-Hydroxytamoxifen
CB: Calbindin-D28K
CBP: Calcium-binding protein
CR: Calretinin
DA: Dopamine
Gad67: Glutamic acid decarboxylase 67
GlyT2: Glycine transporter 2
GFP: green fluorescent protein
HA: Hemagglutinin
PV: Parvalbumin
TBS: Tris-buffered saline
VGluT2: Vesicular glutamate transporter

Table 1: List of drugs

Drugs	Doses	Suppliers	Catalog no
d-amphetamine	10 mg/kg, i.p.	Tocris Bioscience	#2813
Cocaine	15 mg/kg, i.p.	Sigma-Aldrich	#C5776
Methylphenidate	15 mg/kg, i.p.	Sigma-Aldrich	#M2892
GBR12783	15 mg/kg, i.p.	Tocris Bioscience	#0513
Desipramine	15 mg/kg, i.p.	Tocris Bioscience	#3067
Imipramine	10 mg/kg, i.p.	Sigma-Aldrich	#I7379
Morphine	5 mg/kg, s.c.	Tocris Bioscience	#5158
Dizocilpine	0.3 mg/kg, i.p.	Tocris Bioscience	#0924

Table 2: List of primary antibodies

Antigen	Host	Dilution	Supplier	Catalog no
pS32-cFos	Rabbit	1:500	Cell Signaling	#11919
HA	Mouse	1:1000	Covance	#MMS-101R
GFP	Chicken	1:1000	Life Technologies	#A10262
CR	Mouse	1:500	Swant	#6B3
CB	Mouse	1:500	Swant	#300
PV	Mouse	1:500	Swant	#235

HA, hemagglutinin; GFP, green fluorescent protein; CR, calretinin; CB, calbindin-D28k; PV, parvalbumin.

Table 3: Number of cells quantified in the lumbar spinal cord

Figures	Lamina									
	I	II	III	IV	V	VI	VII	VIII	IX	X
Figure 2b										
pS32-cFos/GFP	25	26	53	22	5	2	34	13	0	26
pS32-cFos	71	146	213	144	228	474	755	275	0	189
Figure 2d										
pS32-cFos/GFP	0	0	52	52	117	390	91	52	0	26
pS32-cFos	63	145	270	197	292	706	740	241	0	185
Figure 2f										
pS32-cFos/HA	10	104	71	37	28	52	76	32	0	15
pS32-cFos	36	260	178	108	142	188	192	80	0	45
Figure 2h										
pS32-cFos/CB	3	11	9	3	1	4	2	0	0	3
pS32-cFos	21	152	151	138	151	310	442	233	0	91
Figure 2j										
pS32-cFos/CR	0	22	1	3	4	4	4	4	0	0
pS32-cFos	10	49	251	165	168	398	450	248	0	103
Figure 2l										
pS32-cFos/PV	1	21	8	4	8	13	6	6	0	3
pS32-cFos	13	221	150	105	108	283	481	187	0	130
Figure 3d										
pS32-cFos/GFP	5	72	258	85	49	74	91	19	0	55
GFP	52	218	580	222	148	201	308	53	0	128

GFP, Green Fluorescent Protein; HA, hemagglutinin; PV, Parvalbumin; CB, Calbindin-D28k; CR, Calretinin.

Tarot et al., Figure 1

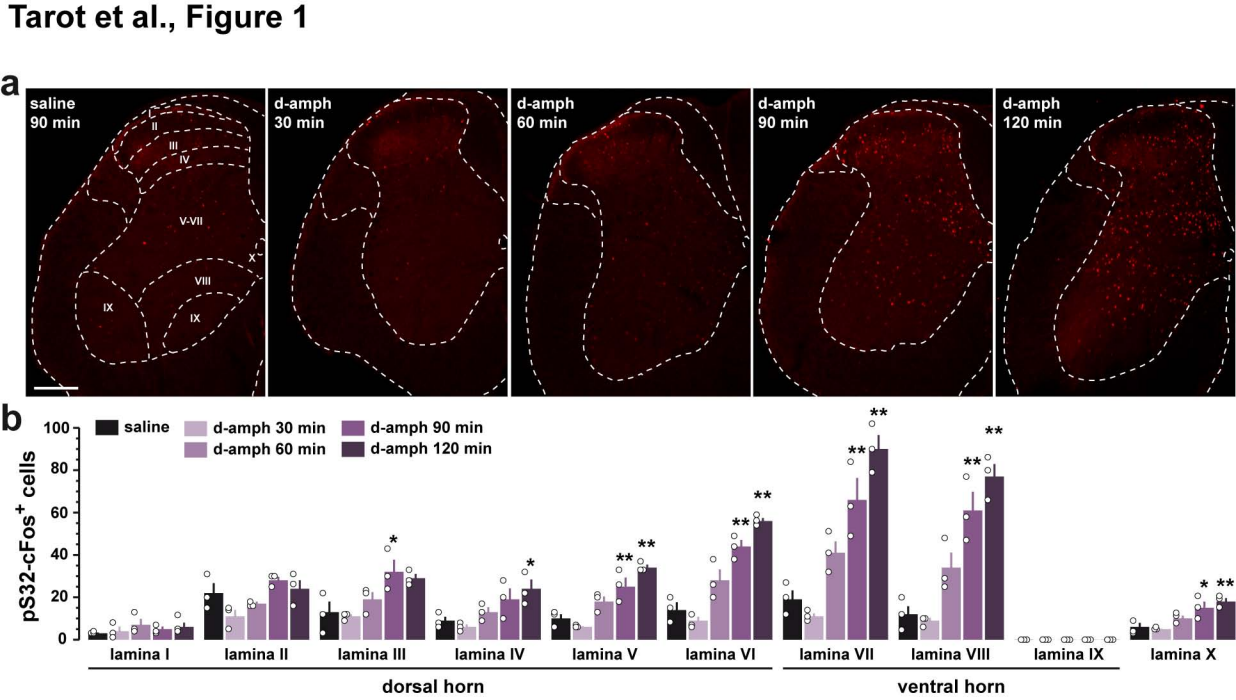

Tarot et al., Figure 2

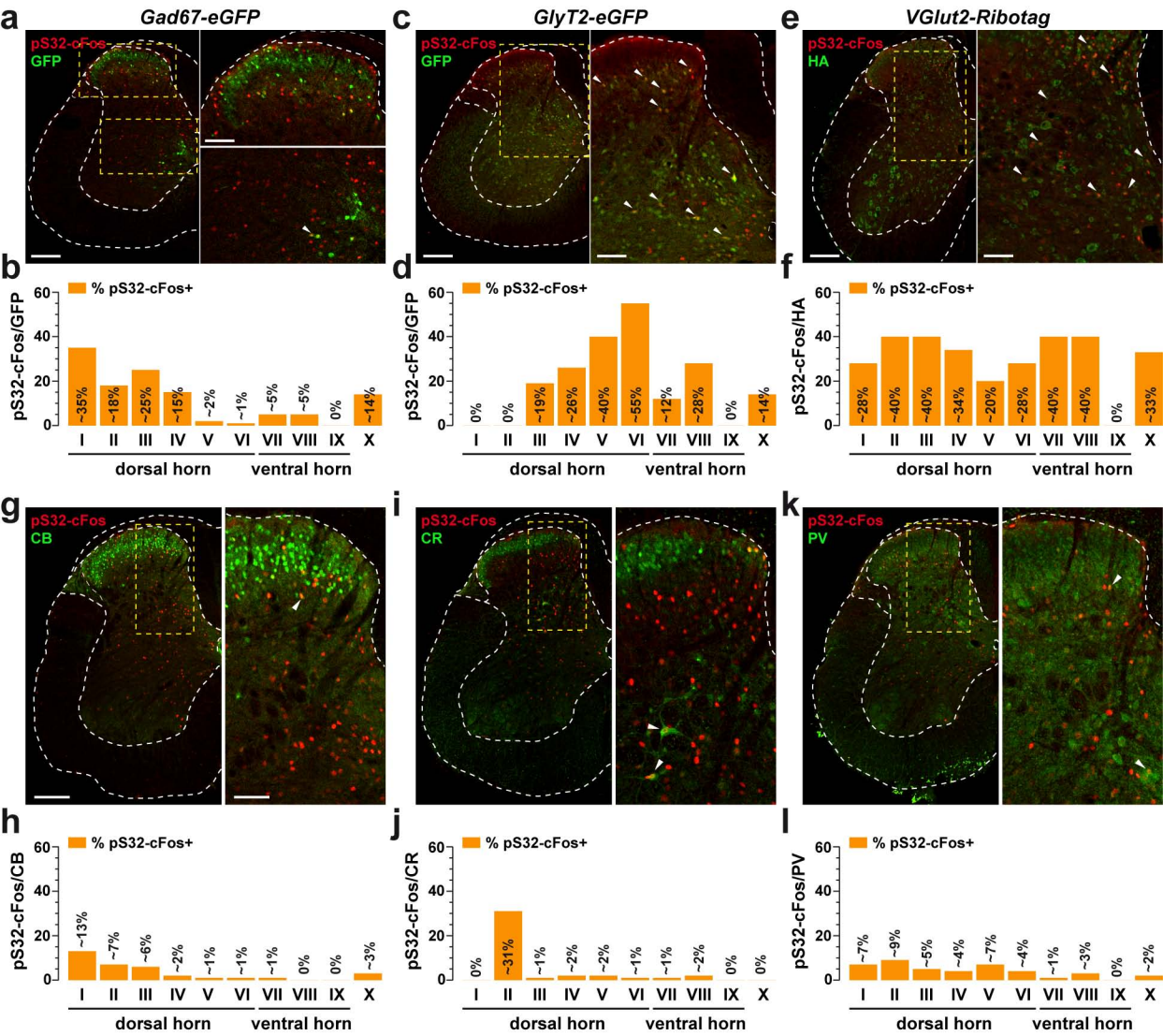

Tarot et al., Figure 3

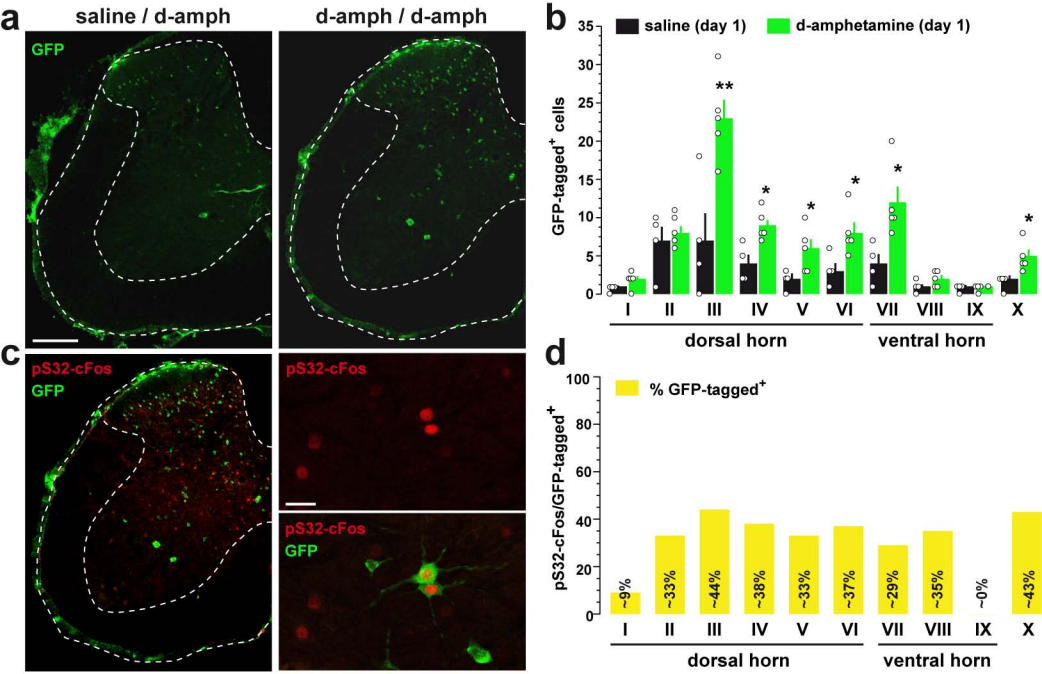

Tarot et al., Figure 4

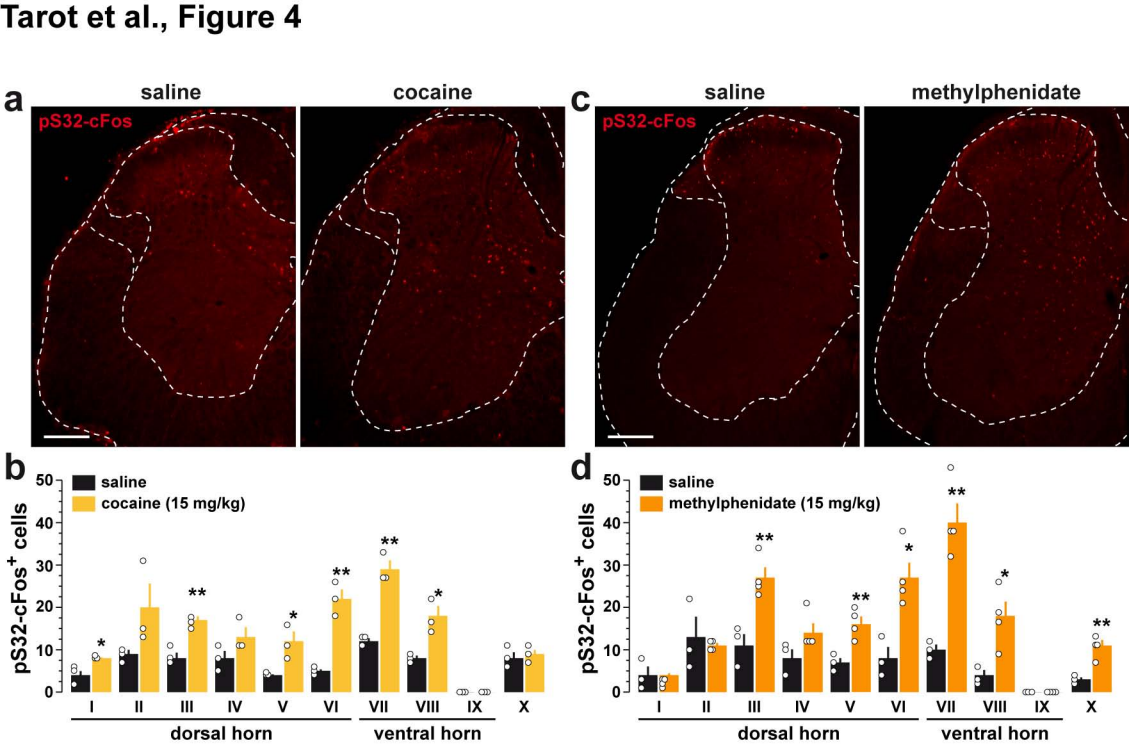

Tarot et al., Figure 5

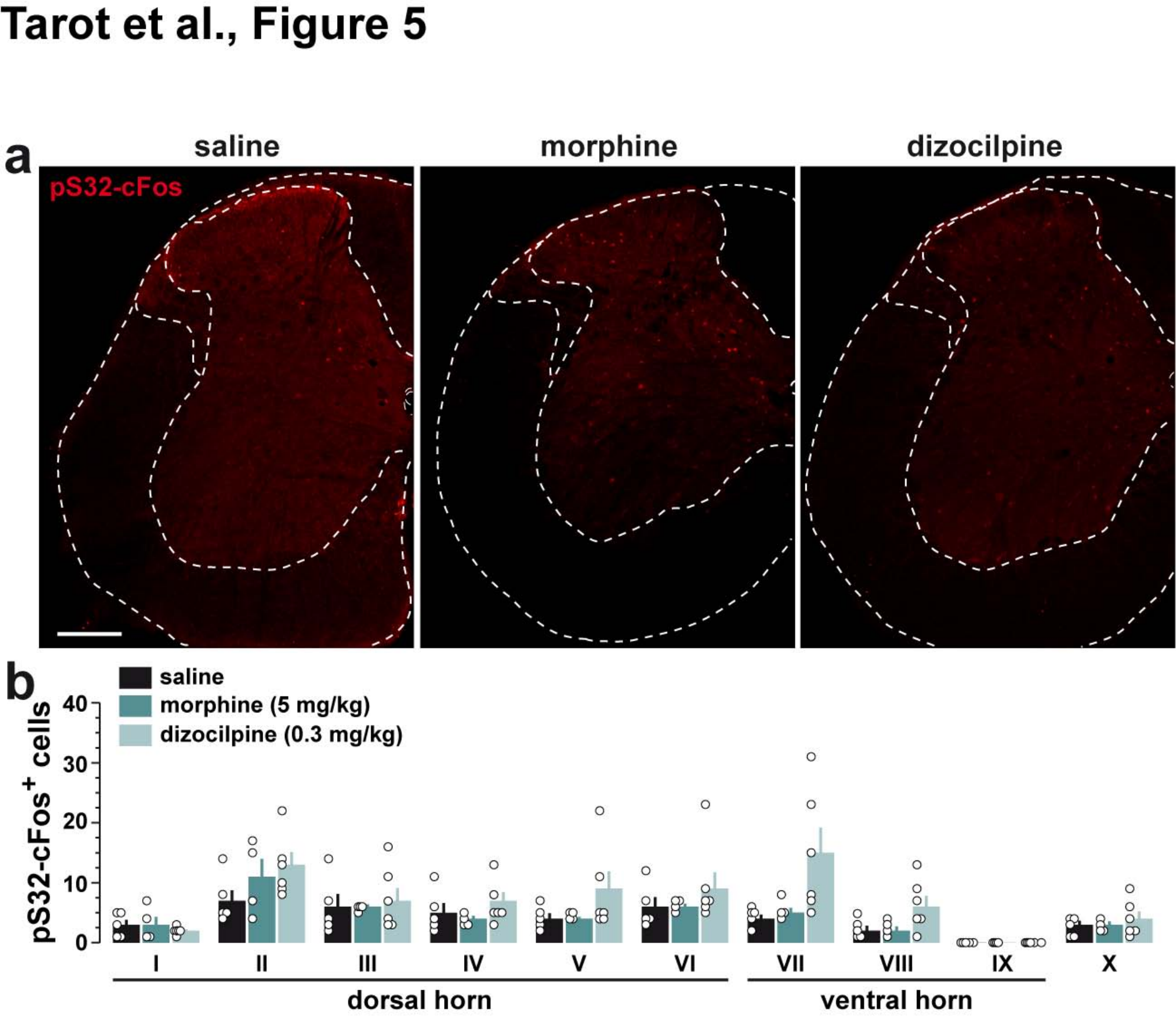

Tarot et al., Figure 6